



# Crustal rheology of the Santorini–Amorgos zone: Implications for the nucleation depth and rupture extent of the 9 July 1956 Amorgos earthquake, southern Aegean

K.I. Konstantinou\*

*Institute of Geophysics, National Central University, Jhongli 320, Taiwan*

## ARTICLE INFO

### Article history:

Received 26 November 2009  
Received in revised form 29 April 2010  
Accepted 9 May 2010

### Keywords:

Rheology  
Strength  
Lithosphere  
Aegean  
Amorgos  
Greece

## ABSTRACT

The 9 July 1956 Amorgos earthquake (Mw 7.6) was the largest event that hit Greece during the last century followed by a tsunami that inundated the coastal areas of the southern Aegean. This study investigates the rheological properties of the 1956 rupture zone between Amorgos and Santorini islands, in an effort to place some constraints on the nucleation depth and rupture extent of this large event. The seismic velocities inferred from tomographic and surface wave dispersion studies of the area are first correlated with laboratory determined velocities of known rock types. It is found that the lithosphere in the southern Aegean can be approximated by three layers representing the upper/lower crust and upper mantle consisting of quartzite, diabase and peridotite, respectively. Geotherms are calculated by using an analytical solution to the one-dimensional heat conduction equation, while Yield Strength Envelopes (YSEs) are produced after assuming laboratory estimated parameters of brittle and ductile deformation for each rock type. The depth frequency of earthquakes in the area, as well as other independent observations favour the YSE calculated for a wet upper crust/upper mantle, a dry lower crust and a geotherm corresponding to a surface heat flow of  $62 \text{ mW m}^{-2}$ . In this YSE, the upper mantle exhibits maximum strength at 33 km becoming more ductile at greater depths. The lower crust retains significant strength and therefore cannot flow as it did during the early stages of extension, but it is relatively weaker than the upper mantle confirming the 'jelly sandwich' model previously proposed for the continental lithosphere. The downdip rupture width of the Amorgos event can be estimated from empirical relationships to be 26 km which means that its rupture may have extended from the depth of peak strength in the upper mantle (33 km) to 7 km upwards. Such a scenario agrees well with recent modelling results indicating that the Amorgos tsunami was probably caused by submarine landslides rather than coseismic rupture of the seafloor.

© 2010 Elsevier Ltd. All rights reserved.

## 1. Introduction

It is still hotly debated whether the strength of the continental lithosphere mostly resides in the upper mantle or in the seismogenic part of the crust. The former suggestion widely known as the 'jelly sandwich' model, predicts that continental lithosphere consists of the upper crust and mantle that are strong, separated by a weak lower crust (Chen and Molnar, 1983; Ranalli and Murphy, 1987; Handy and Brun, 2004; Burov and Watts, 2006). This model has been used during the last two decades in order to explain the rheological stratification of continental lithosphere and the depth frequency of earthquakes (e.g., Déverchère et al., 2001). The latter suggestion (dubbed as 'crème brûlée' model) appeared

more recently when a re-assessment of focal depth distribution in southern Iran, Tien Shan and northern India showed a complete absence of seismicity in the continental mantle (Maggi et al., 2000a,b; Jackson, 2002; Priestley et al., 2008). Based on this model, the lack of seismicity in the upper mantle clearly implies that it is actually weak while most of the strength lies in the upper and lower crust that are seismogenic. However, taking into account that different continental lithospheres have different composition and tectonothermal history, it is more likely that these two models may be the end members of a whole range of rheological behaviour (Afonso and Ranalli, 2004).

The southern Aegean is an area affected by the subduction of the African lithosphere at a rate of about  $1 \text{ cm yr}^{-1}$  while the upper Aegean plate moves towards SW at  $3.5 \text{ cm yr}^{-1}$  (Fig. 1) (McClusky et al., 2000). The result of this subduction process is a well-defined Wadati-Benioff zone and the occurrence of volcanism that is expressed through a number of active volcanic centers

\* Fax: +886 3 4222044.

E-mail address: [kkonst@ncu.edu.tw](mailto:kkonst@ncu.edu.tw).

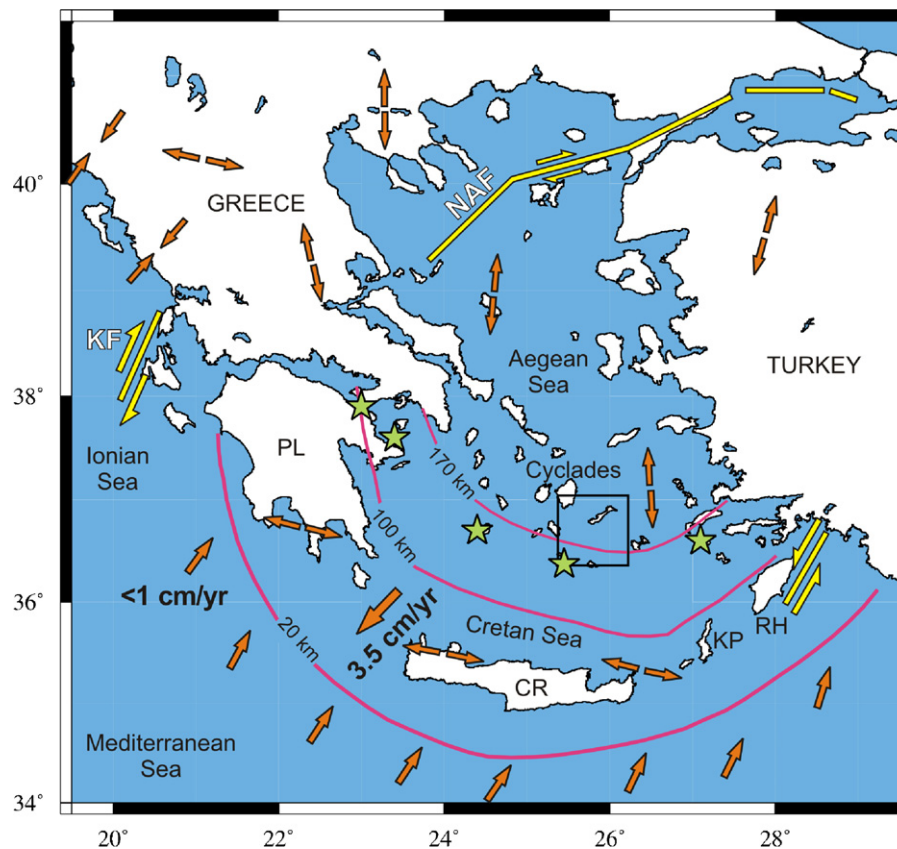


**Fig. 1.** Map of the Greek region showing the main tectonic characteristics of the area adopted from Papazachos and Papazachou (1997); Papazachos et al. (2000). Single arrows indicate the plate motion direction along with average rate of convergence per year after McClusky et al. (2000). Double arrows indicate the areas where either extension (arrows in opposite directions) or compression (arrows facing each other) prevails. Thick yellow lines represent the main strike-slip fault zones. The curves for 20, 100 and 170 km are isodepth curves showing the hypocentral depth distribution of earthquakes occurring along the Wadati-Benioff zone. The green stars are the locations of active volcanoes. The square shows the area of interest between Amorgos and Santorini islands. PL: Peloponnese, CR: Crete island, KP: Karpathos island, RH: Rhodes island, KF: Kefalonia Fault, and NAF: North Anatolian Fault. (For interpretation of the references to color in the figure caption, the reader is referred to the web version of the article.)

extending from the Peloponnese eastwards to the Turkish coast. Geodetic as well as seismologic observations indicate the dominance of extensional deformation throughout the Aegean region that has started since the Oligocene, modified by the westward movement of the Anatolian plate in the late Miocene (Le Pichon and Angelier, 1979; Le Pichon et al., 1995). Extension was most likely the result of gravitational collapse of a previously thick and hot lithosphere and it was also responsible for the exhumation of HP metamorphic rocks that form today the Cyclades islands core complex (Brun and Faccenna, 2008). This extensional regime has caused considerable thinning of the crust in the southern Aegean and several studies indicate a thickness of about 25 km (Tirel et al., 2004; Karagianni et al., 2005; Sodoudi et al., 2006; Endrun et al., 2008).

On 9 July 1956 a large earthquake occurred near the Cyclades island of Amorgos causing extensive damage to the nearby area while 53 people were killed and 100 were injured (Papazachos and Papazachou, 1997; Schenková et al., 2005). The event was followed by a tsunami which started from SE of Amorgos and inundated the coasts of neighbouring islands having heights of 20–25 m also reaching the Turkish coast (Papazachos et al., 1985). More recently, Okal et al. (2009) inverted historical seismograms of the Amorgos earthquake in order to obtain its focal mechanism and also produced refined epicenters for some of the aftershocks (Fig. 2). The inferred seismic moment for the Amorgos event ( $3.9 \times 10^{27}$  dyn-cm) corresponds to a moment magnitude of 7.6, which makes this earthquake the largest one to hit Greece in the last century. Its centroid depth was estimated to lie inside the upper mantle at 45 km depth. The authors support this relatively large depth by numeri-

cal modelling of the tsunami generation and propagation showing that it was most probably caused by submarine landslides triggered by the mainshock, rather than coseismic rupture of the seafloor. The aforementioned results imply that the upper mantle around Amorgos is strong and that the 'jelly sandwich' model can possibly describe the rheology of this area. However, to date there has not been any study examining in detail the lithospheric strength of Santorini–Amorgos zone and whether it can provide any constraint on the nucleation depth and rupture extent of the 1956 earthquake.

This work investigates the rheological conditions near the rupture zone of the 1956 Amorgos earthquake in an effort to clarify these issues. First, all the available information for this area is presented such as crustal and upper mantle structure, seismicity and depth distribution of earthquakes as well as geodetically determined strain rates. Then the temperature distribution as a function of depth is calculated using an analytical solution to the heat conduction equation and lithospheric strength is estimated assuming a three-layer compositional model (upper crust, lower crust, upper mantle). Finally, this study concludes with a discussion of the results and their implications for 1956 earthquake and lithospheric dynamics in the southern Aegean.

## 2. Salient features of the area

### 2.1. Crustal and upper mantle structure

The Aegean area has been recently the focus of extensive research regarding its crustal and upper mantle structure in order

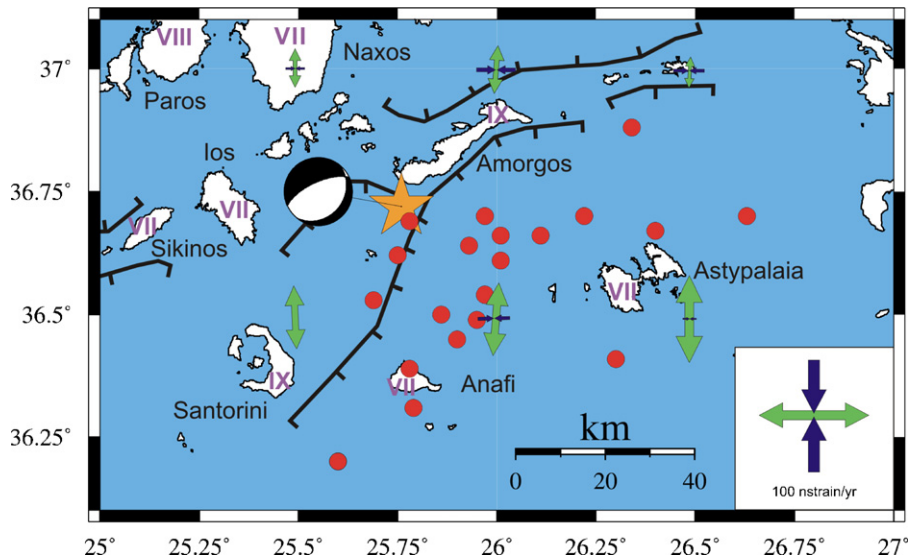


**Fig. 2.** Map of the area where the 1956 Amorgos earthquake occurred. The star indicates the epicenter of the Amorgos mainshock, while the red circles are aftershock epicenters taken from Okal et al. (2009). The beachball represents the focal mechanism of the mainshock inferred from moment tensor inversion of historical seismograms performed by Okal et al. (2009). Roman numerals shown on the nearby islands are intensity estimates for the mainshock according to the Modified Mercalli intensity scale (from Schenková et al., 2005). Black thick lines indicate normal faults in the area adopted from Bohnhoff et al. (2006). Double arrows represent principle axes of the strain rate tensor for this area determined from GPS data (from Hollenstein et al., 2008). (For interpretation of the references to color in the figure caption, the reader is referred to the web version of the article.)

to obtain a better understanding of subduction geometry and processes. Tomographic images (Papazachos and Nolet, 1997) confirmed earlier results from active source experiments (e.g., Makris, 1978) about the thinning of the crust in the southern Aegean and the relatively flat Moho. The use of receiver functions that are more sensitive in detecting such velocity discontinuities, made possible an accurate assessment of the Moho depth at 24–27 km around the area of Cyclades and Cretan Sea while it was found at 34 and 24 km in western and eastern Crete respectively (Knapmeyer and Harjes, 2000; Li et al., 2003; Endrun et al., 2004; Sodoudi et al., 2006; Zhu et al., 2006). These results also agree in general with Moho estimates obtained from modelling of gravity data (Tsokas and Hansen, 1997; Tirel et al., 2004). The crust itself seems to be partitioned in an upper and lower part with their boundary lying at about 15 km depth, as has been shown by a seismic reflection survey in the Cyclades where a layered lower crust was found (Sachpazi et al., 1997).

The study of surface wave dispersion can provide estimates of the absolute shear wave velocity as a function of depth and several such studies exist now for the southern Aegean (Karagianni et al., 2005; Di Luccio and Pasyanos, 2007; Endrun et al., 2008). According to these studies the upper crust (0–15 km) exhibits average velocities in the range 3.3–3.4 km s<sup>-1</sup> and is covered by a variable thickness layer of loose sediment ( $V_s \sim 1\text{--}2$  km s<sup>-1</sup>). The velocities in the lower crust (15–25 km) can range from 3.5 to 3.9 km s<sup>-1</sup>, but most studies indicate that they are higher than 3.7 km s<sup>-1</sup>. Using a mean  $V_p/V_s$  ratio of 1.74 that was determined for the Cyclades islands by Zhu et al. (2006) it is possible to convert the shear wave velocities into  $V_p$  and compare these values with laboratory determined ones compiled by Christensen and Mooney (1995) for a variety of rock types. In this way, the upper crust (5.7–5.9 km s<sup>-1</sup>) corresponds either to quartzite or granitic gneiss, while the lower crust (6.5–6.6 km s<sup>-1</sup>) has velocities compatible with diabase or mafic granulite.

Differences can be found among the aforementioned studies when upper mantle shear wave velocity is considered. Karagianni et al. (2005) reports that  $V_s$  just below the Moho (26–30 km) has a value of 4.2 km s<sup>-1</sup> but at greater depths (30–40 km) it is reduced to 3.8 km s<sup>-1</sup>. This finding conflicts with the results of the other two studies that indicate shear velocity at depths 26–60 km is between

4.3–4.5 km s<sup>-1</sup>. Endrun et al. (2008) attribute this difference partly to the model parametrizations used in each study and partly to the limited resolution below 30 km of the group velocity study of Karagianni et al. (2005). Results of Pn tomography seem to support the observations of high  $V_s$  beneath the southern Aegean upper mantle, since it is found that Pn velocity is of the order of 8.2 km s<sup>-1</sup> (Al-Lazki et al., 2004). Subduction zones are areas where ascending fluids from slab dehydration and metamorphic reactions can have a great impact on the seismic velocities in the mantle wedge. Fig. 3 shows laboratory determined shear wave velocities of peridotite as a function of increasing degree of alteration obtained at pressures appropriate for the base of 25 km thick crust. It can be seen that only the value of Karagianni et al. (2005) is consistent with

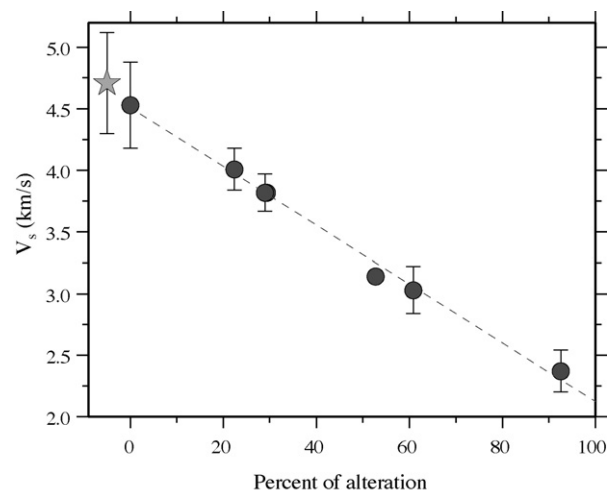


**Fig. 3.** Diagram showing the distribution of peridotite shear wave velocities as a function of increased alteration due to contamination with water-bearing minerals for a pressure appropriate at the base of a 25 km thick crust (from Christensen, 1966). The dashed line is the least-squares fit to the data points, while the vertical error bars represent velocity variations due to anisotropic effects. The star is the shear wave velocity of pure dunite and is given here for comparison. The zero point of the x-axis is shifted to the right for clarity.

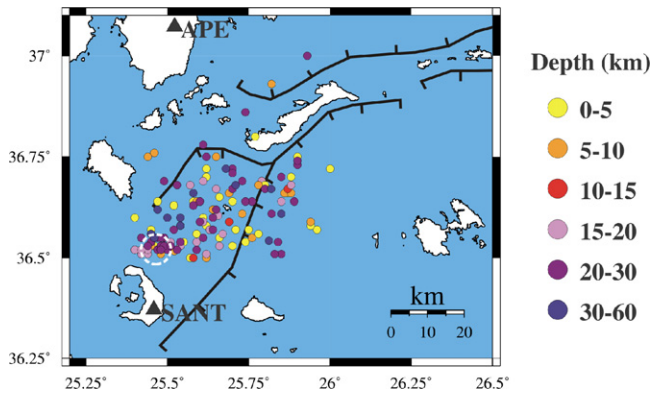


**Fig. 4.** Map showing the distribution of event locations taken from the NOA catalogue for the period January 2000 until September 2009 (see text for more details). Hypocentral depths follow the color scale shown at the right hand side of the plot. Also shown are the locations (black triangles) of the two closest stations APE and SANT. The white dashed line indicates the location of Columbo reef, a submarine volcanic structure related to the Santorini volcanic center. Other symbols same as in Fig. 2. (For interpretation of the references to color in the figure caption, the reader is referred to the web version of the article.)

larger degrees of alteration, while all other velocities suggest that the upper mantle probably consists of almost unaltered peridotite at depths shallower than 60 km.

## 2.2. Seismicity and earthquake depths

The seismicity catalogue of the National Observatory of Athens (NOA) (available from <http://www.gein.noa.gr>) covers several decades and is the primary source of information about earthquake occurrence in the Greek region. For the purpose of this study and in order to insure the accuracy of earthquakes locations only the part of the catalogue that starts from the year 2000 until present will be used. The reasoning behind this choice lies in the fact that in the late 1990s NOA started upgrading its seismic network by replacing analogue stations with digital ones and short-period sensors with broadband (for a more detailed description see Melis and Konstantinou, 2006). More importantly, station APE was upgraded to digital and station SANT was installed on Santorini island in collaboration with GFZ Potsdam in the late 1990s considerably improving the location accuracy around the Amorgos area (see Fig. 4). Routine processing of recorded events by NOA staff includes manual picking of P- and S-phases and location using a version of HYPO71 (Lee and Lahr, 1975) assuming a 1D velocity model derived from the tomography results of Papazachos and Nolet (1997). Except from seismicity occurring in the upper plate, the area around Amorgos also experiences earthquakes with hypocentral depths larger than 100 km owing to the ongoing subduction of the African slab. This study only focuses on events with hypocentral depths shallower than 60 km, therefore all subduction-related events are excluded from further analysis.

Initially the NOA catalogue was searched and events located near the rupture area of the 1956 earthquake were obtained along with their picked phases and location uncertainties. This dataset was screened in order to remove any outliers using the following criteria: (a) P- and S-phase from at least one of the two closest stations (APE, SANT) were used in the travel time inversion for the location, (b) *rms* residuals were smaller than 1.0 s, and (c) the location error did not exceed 5 km horizontally and vertically. The first criterion is based on the suggestion of Gombert et al. (1990) that at least one P- and one S-phase is needed at a station with a distance of 1.5 focal depths from the source for a reliable location. In this way 139 events were finally obtained for the period starting January 2000 until September 2009 recorded by at least

5 stations. The global relocation database of Engdahl et al. (1998) was also searched for the period prior to 2000, however, only three events were flagged as well-constrained ('DEQ' flag which means that the teleseismic azimuthal gap is less than 180° and all parameters were free during the travel time inversion). A map view of the location of all 142 events can be seen in Fig. 4 where it is clear that most of the seismicity falls in the area between the two islands (Amorgos–Santorini). A histogram of the depth distribution of these events using a bin size proportional to the maximum location error (5 km), reveals one peak inside the upper crust (~5 km) and a second one around the Moho (~25 km) (Fig. 5a). After about 35 km depth seismicity levels drop sharply and there are almost no events located deeper than 50 km. Also shown in the histogram is the centroid depth (45 km) for the 1956 event estimated by Okal et al.

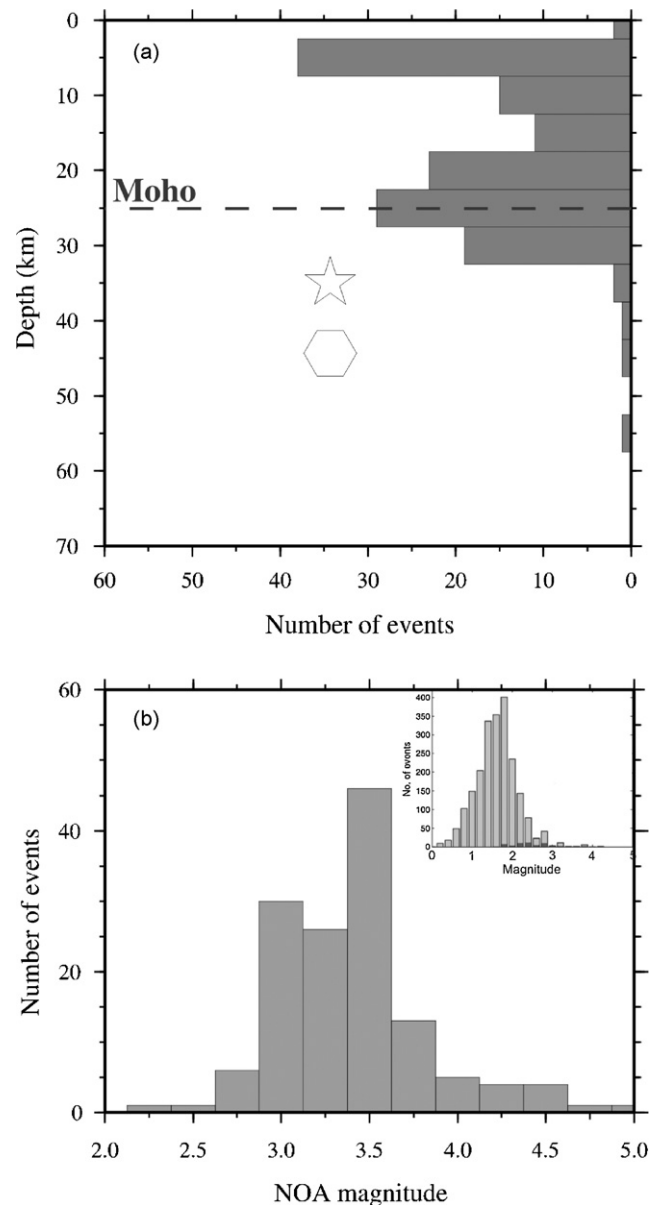


**Fig. 5.** (a) Histogram showing the distribution of hypocentral depths for the 142 events that are considered in this study. The dashed line highlights the Moho depth in the Amorgos area. The star indicates the hypocenter according to the Engdahl et al. (1998) catalogue, while the hexagon indicates the centroid depth for the 1956 earthquake reported by Okal et al. (2009) and (b) distribution of magnitudes for the NOA catalogue events; the inset at the upper right hand corner shows the magnitude distribution for events recorded by a temporary seismic network in the Cyclades islands (from Bohnhoff et al., 2006).

(2009) and the hypocentral depth (35 km) according to Engdahl et al. (1998), who have flagged it as 'AFEQ'. This means that the teleseismic azimuthal gap is more than 180° and the depth was fixed to 35 km during the travel time inversion, resulting in a poorly constrained location.

Recently, Bohnhoff et al. (2006) have conducted a microearthquake survey in the area of the Cyclades islands covering also the rupture zone of the 1956 event. The authors found that seismicity occurs at the same area between Santorini and Amorgos islands as indicated by the NOA catalogue and most events concentrate at 5–9 km depth with few of them originating deeper. Most of the shallow seismicity adjacent to Santorini is associated with the Columbo reef, a volcanic submarine structure that exhibits strong hydrothermal activity. These events have magnitudes smaller than 3.0 and in most cases smaller than 2.0 (Fig. 5b inset), typical for events caused by the ascent and circulation of volcanic fluids inside the upper crust. Events deeper than 20 km were relatively scarce in the seismicity observed by Bohnhoff et al. (2006) which is apparently in conflict with the depth distribution of NOA locations shown in Fig. 5a. The reason for this difference probably lies in the limited time period (22 months) of the microearthquake survey that resulted in the recording of a large number of shallow, small magnitude events. On the contrary, the events listed in the NOA catalogue have in most cases magnitudes larger than 3.0 (Fig. 5b) as a result of the detection threshold of the NOA network. Also, deeper events occur at a rate of 4–10 per year in the NOA catalogue and therefore would not contribute much to the observed seismicity recorded by a short-term deployment. Obviously, the NOA catalogue includes events over a time span of almost 9 years and is therefore more representative of the long-term strength of the lithosphere.

### 2.3. Geodetic strain rates

Primarily campaign but also continuous GPS measurements have been used previously to determine the crustal motion in the area of the southern Aegean (Kremer and Chamot-Rooke, 2004; Hollenstein et al., 2008). There is a general agreement among authors that the area of western Cyclades deforms very slowly and the estimated strain rate does not exceed 5 n strain yr<sup>-1</sup>. The situation is completely different in the eastern Aegean and in the area of the 1956 Amorgos earthquake where strain rates attain values of about 50 n strain yr<sup>-1</sup>. Fig. 2 shows this progressive increase of strain rates from the island of Naxos in the NW, to Amorgos and Astypalaia islands in the SE. As already discussed the principal axes of the strain tensor indicate an almost purely extensional deformation with a N-S direction in the area of Amorgos.

### 3. Calculation of geotherms

The distribution of temperature as a function of depth inside the Earth can be described by the one-dimensional equilibrium heat conduction equation. This equation is given by

$$\frac{\partial^2 T}{\partial z^2} = -\frac{A}{k} \quad (1)$$

where  $T$  is temperature,  $z$  is the depth,  $A$  the radiogenic heat generation rate per unit volume and  $k$  the thermal conductivity. Two boundary conditions are needed in order to solve this second-order partial differential equation, one that specifies that at depth  $z = 0$  the surface heat flow  $Q_0$  is equal to  $-k\partial T/\partial z$  and that  $T = T_0$  at  $z = 0$ . If a layered model is assumed then each layer  $i$  has a constant thermal conductivity  $k_i$  and radiogenic heat generation rate  $A_i$ . Then the temperature  $T_{n,z}$  in layer  $n$  at depth  $z$  is (e.g., Aldersons et al., 2003)

**Table 1**

Thermophysical parameters for the different lithologies considered in this study. Values are taken from Afonso and Ranalli (2004) and references therein. Density values are also consistent with those inferred from modelling of gravity data in the southern Aegean by Casten and Snopek (2006).

Layer	$A$ ( $\mu\text{W m}^{-3}$ )	$K$ ( $\text{W m}^{-1} \text{K}^{-1}$ )	Density ( $\text{kg m}^{-3}$ )
Wet quartzite	1.4	2.5	2640
Dry diabase	0.4	2.1	2850
Wet diabase	0.4	2.1	2850
Peridotite	0.006	3.0	3320

$$T_{n,z} = -\frac{A_n}{2k_n}z^2 + \left[ \sum_{i=1}^{n-1} \left( \frac{A_{i+1}}{k_{i+1}} - \frac{A_i}{k_i} \right) z_i + \frac{Q_0}{k_1} \right] z + \sum_{i=1}^{n-1} \left( \frac{A_i}{2k_i} - \frac{A_{i+1}}{2k_{i+1}} \right) z_i^2 + T_0 \quad (2)$$

where  $z_i$  is the bottom of layer  $i$  and the negative sign signifies that temperature increases downwards. This one-dimensional geotherm is quite sensitive to the choice of the surface heat flow  $Q_0$ .

In order to estimate the temperature distribution using the methodology outlined above, three layers are assumed: one for the upper crust, lower crust and upper mantle respectively. Based on the correlation between seismic velocities and lithology described in Section 2.2 the upper crust is assumed to consist of quartzite, the lower crust of diabase and the upper mantle of peridotite. Such a configuration is also consistent with densities inferred from modelling of gravity data for the southern Aegean (Casten and Snopek, 2006). Table 1 lists the values of heat production and thermal conductivity for the different lithologies considered here while the surface temperature was assumed equal to 15 °C. Even though the surface heat flow is the most important parameter in these calculations, there is very little information concerning heat flow measurements in the southern Aegean. Jongsma (1974) conducted such measurements in selected locations in the Cretan Sea and north of the Cyclades islands. The closest of these locations to Amorgos island lies south of Santorini (35°44.1'N, 25°17.4'E) and indicates a surface heat flow of 62 mW m<sup>-2</sup>. On the other hand, Makris and Stobbe (1984) have presented a heat flow map for the Aegean region where they indicate that surface heat flow in the Santorini–Amorgos area is higher than 67 mW m<sup>-2</sup>. Fig. 6 shows

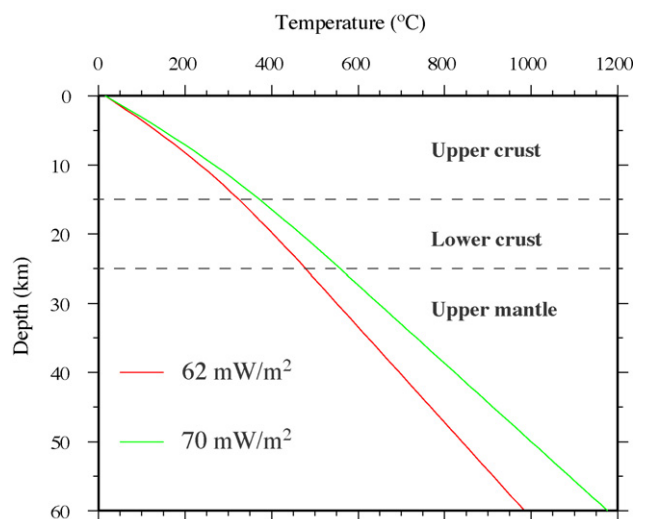


**Fig. 6.** Diagram showing the variation with depth of the two geotherms calculated for different surface heat flow values. Also shown are the upper/lower crust and lower crust/upper mantle boundaries.

two calculated geotherms, one corresponding to a surface heat flow value of  $62 \text{ mW m}^{-2}$  and the other for a value of  $70 \text{ mW m}^{-2}$ . For comparison purposes both of these calculated geotherms will be used in the rheological modelling described later.

#### 4. Rheological modelling

A rheological profile or Yield Strength Envelope (YSE) is a curve that depicts the distribution of differential stress as a function of depth and has been used extensively as an estimate of the mechanical strength of the lithosphere (e.g., Lamontagne and Ranalli, 1996; Déverchère et al., 2001; Aldersons et al., 2003; Ma and Song, 2004; Solaro et al., 2007; Fernández-Ibañez and Soto, 2008; Albaric et al., 2009 among others). The part of the curve that corresponds to the brittle behaviour of the lithosphere is expressed by a linear friction failure law given by

$$(\sigma_1 - \sigma_3) = \beta \rho g z (1 - \lambda) \quad (3)$$

where  $\sigma_1$ ,  $\sigma_3$  are maximum and minimum compressive stress,  $\rho$  is the density of the material,  $g$  is acceleration due to gravity,  $z$  is the depth,  $\lambda$  is pore-fluid pressure and  $\beta$  is a parameter that depends on the type of faulting. Ductile behaviour of the lithosphere is temperature dependent and is expressed by a power-law creep that is

$$(\sigma_1 - \sigma_3) = \left( \frac{\dot{\epsilon}}{A} \right)^{1/n} \exp \left( \frac{Q}{nRT(z)} \right) \quad (4)$$

where  $\dot{\epsilon}$  is the strain rate,  $A$  and  $n$  are creep parameters of the material,  $Q$  is the activation energy for creep,  $R$  is the gas constant ( $8.314 \text{ J K}^{-1} \text{ mol}^{-1}$ ) and  $T(z)$  is the temperature as a function of depth. At this point it should be noted that the rheological modelling described above contains many sources of uncertainties (like possibility of a non-steady thermal regime, variations in the heat production in the crust, uncertainties of the thermophysical/creep parameters assumed) that may lower the accuracy of the calculated YSEs. It is generally accepted however, that these YSEs can provide a useful first-order approximation to the actual rheological variation of the lithosphere as attested by the studies cited earlier.

A model of three layers with the same assumed lithologies as in the calculation of the geotherm is again used (i.e. upper crust-quartzite, lower crust-diorite, upper mantle-peridotite) for the rheological modelling. The brittle part is calculated by using a near hydrostatic pore-fluid pressure ( $\lambda = 0.4$ ) and  $\beta = 0.75$  appropriate for normal faulting since the area of Amorgos experiences extensional deformation. A strain rate  $\dot{\epsilon} = 1.58 \times 10^{-15} \text{ s}^{-1}$  is used for the ductile part calculations, in agreement with the geodetic strain rates for the Amorgos area. Even small amounts of water can change the rheological behaviour of Earth materials significantly, therefore it should be determined whether the assumed lithologies are considered as wet or dry. The upper crust in the area of the 1956 event lies underneath the sea and rheological parameters consistent with wet quartzite is the most reasonable choice. However, the problem of fluid content in the upper mantle is not so well understood, even though the upper mantle above subduction zones is assumed to be wet (e.g., Afonso and Ranalli, 2004). Also, it is not clear whether the lower crust beneath the southern Aegean can be considered as dry or wet. Taking into account these difficulties, different YSEs have been calculated using all possible combinations of wet and dry lower crust/upper mantle rheologies (Fig. 7). Table 2 summarizes all the rheological parameters of the lithologies used in this study for both dry and wet cases.

## 5. Discussion

### 5.1. Crustal rheology and the Amorgos earthquake

The calculated YSEs suggest that mainly two factors play the most important role in the depth distribution of lithospheric strength in the Amorgos area. The first is the assumed geotherm (which in turn depends on the surface heat flow) that may shift the brittle–ductile transition depth in the upper mantle to shallower or larger depths. Assuming a wet upper mantle rheology along with high surface heat flow leads to a considerable shrinking of the mantle strength to the depths just below the Moho. This is not the case when a dry rheology is assumed, but as mentioned earlier such an assumption may not be realistic for the upper mantle above an active subduction zone. The second factor has to do with the rheology of the lower crust and whether it can be considered as dry or wet. A wet rheology consistently generates brittle–ductile transition zones between the lower crust and upper mantle that could function as decoupling horizons between the two lithological units (Ranalli, 1995). On the contrary, a dry lower crust model does not produce such zones and predicts a mechanical coupling of the two layers. These factors affect of course very little the upper crust where the brittle–ductile transition starts at about 7–8 km in all of the four YSEs implying some decoupling with the lower crust and upper mantle.

The depth distribution of seismicity presented in Section 2.2 seems to be better fit by the rheological model of a dry lower crust, wet upper mantle and a surface heat flow of  $62 \text{ mW m}^{-2}$  (Fig. 7a). This model can explain both the two peaks of seismicity at about 5 and 25 km and also the sharp decrease at 15 km and at depths larger than 35 km. However, seismicity is not the only set of observations that favours such a rheological model. Jolivet et al. (2009) examined the relationship of SKS-splitting fast directions with the striations observed on exhumed rocks of the metamorphic core complex at some of the Cyclades islands. The authors found that in most cases these two directions were parallel, indicating that the deformation in the lower crust is driven by the flow imposed by the upper mantle during slab retreat while the upper crust is partly decoupled. The geochemistry of lavas erupted from the Santorini volcanic center suggests significant contamination of the original magma with upper crustal material (Zellmer et al., 2000). One reason why the contamination was limited to the upper crust may be that the lower crust was dry and therefore unsuitable to melt and contaminate the rising magma (Annen and Sparks, 2002). It should be noted that in this rheological model even though the lower crust retains significant strength, it is still weaker than the upper mantle thus resembling the ‘jelly sandwich’ model as explained by Burov and Watts (2006).

Based on the rheological model presented here it is possible to put forward a rupture scenario for the Amorgos earthquake. The length  $L$  and downdip width  $W$  of the rupture zone can be estimated by using the empirical relationships (Wells and Coppersmith, 1994)

$$\log L = -2.44 + 0.59M \quad (5)$$

$$\log W = -1.01 + 0.32M \quad (6)$$

where  $M$  is the moment magnitude of the event and setting  $M = 7.6$  yields a length of 110 km and downdip width of about 26 km. Large earthquakes such as the Amorgos event, usually nucleate near the base of the seismogenic layer (Sibson, 1984) therefore the hypocenter can be put near the depth of maximum strength ( $\sim 33$  km). In this way the rupture may have propagated up to a depth of about 7 km which marks the brittle–ductile transition zone of the upper crust (Fig. 8). According to this scenario the rupture does not reach the surface and this agrees with the modelling results of Okal et al. (2009) that indicate that submarine landslides triggered by the

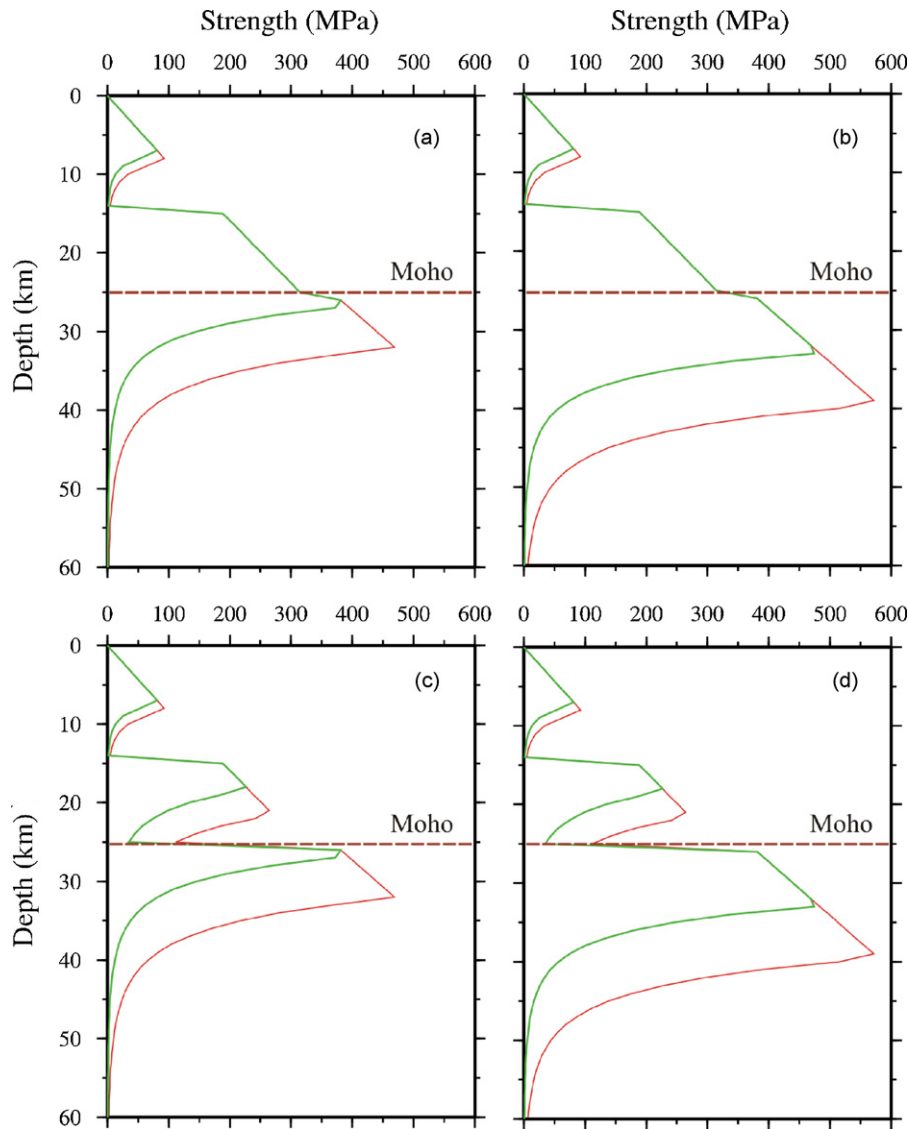


**Fig. 7.** YSEs estimated for different combinations of wet/dry rheologies for the lower crust and upper mantle and for two different geotherms (colours are the same as in Fig. 6): (a) dry lower crust/wet upper upper mantle, (b) dry lower crust/dry upper mantle, (c) wet lower crust/dry upper mantle, (d) wet lower crust/wet upper mantle. (For interpretation of the references to color in the figure caption, the reader is referred to the web version of the article.)

earthquake were responsible for the tsunami that followed, rather than coseismic displacement of the seafloor. These results suggest that a deeper source for the Amorgos earthquake is possible in rheological terms and its centroid can be placed tentatively at 20 km. However, this value is still much shallower than the centroid depth of 45 km reported previously by Okal et al. (2009).

### 5.2. Thermal conditions near the Amorgos rupture zone

The rheological profiles presented earlier along with the observed depth frequency of earthquakes point to the possibility

that the surface heat flow in the area of the 1956 Amorgos event is not as high as previously thought. Xenolith data could be used in order to constrain geotherms and surface heat flow values, however, the author of this article is not aware of any such published data for the Aegean. Nevertheless there are two other ways that can help indirectly constrain the thermal conditions in the area around Amorgos. The first has to do with the  $Pn$  velocity in the upper mantle that can be correlated with the temperature at the Moho  $T_m$  using the relationship (Black and Braile, 1982)

$$Pn = 8.546 - 0.000729T_m \quad (7)$$

for  $Pn$  around  $8.2 \text{ km s}^{-1}$  as determined by Al-Lazki et al. (2004) for the southern Aegean, this relationship implies a Moho temperature of  $470^\circ\text{C}$ . This is in good agreement with the temperature at the Moho assuming a surface heat flow of  $62 \text{ mW m}^{-2}$  ( $T_m = 478^\circ\text{C}$ ), but not with the Moho temperature calculated with  $70 \text{ mW m}^{-2}$  that is  $558^\circ\text{C}$ . The second way is a comparison with the results of Tesaro et al. (2009) who obtained a detailed thermal model of the European lithosphere by inverting a three-dimensional seismic velocity model covering the whole of Europe. For the southern Aegean and at a depth of 60 km their thermal model predicts tem-

**Table 2**

Creep parameters for lithospheric rocks considered in this study. Values are taken from Afonso and Ranalli (2004) and references therein.

Layer	$A \text{ (MPa}^{-n} \text{ s}^{-1}\text{)}$	$n$	$E \text{ (kJ mol}^{-1}\text{)}$
Wet quartzite	$3.2 \times 10^{-4}$	2.3	154
Dry diabase	8.0	4.7	485
Wet diabase	$2.0 \times 10^{-4}$	3.4	260
Dry peridotite	$2.5 \times 10^4$	3.5	532
Wet peridotite	$2.0 \times 10^3$	4.0	471

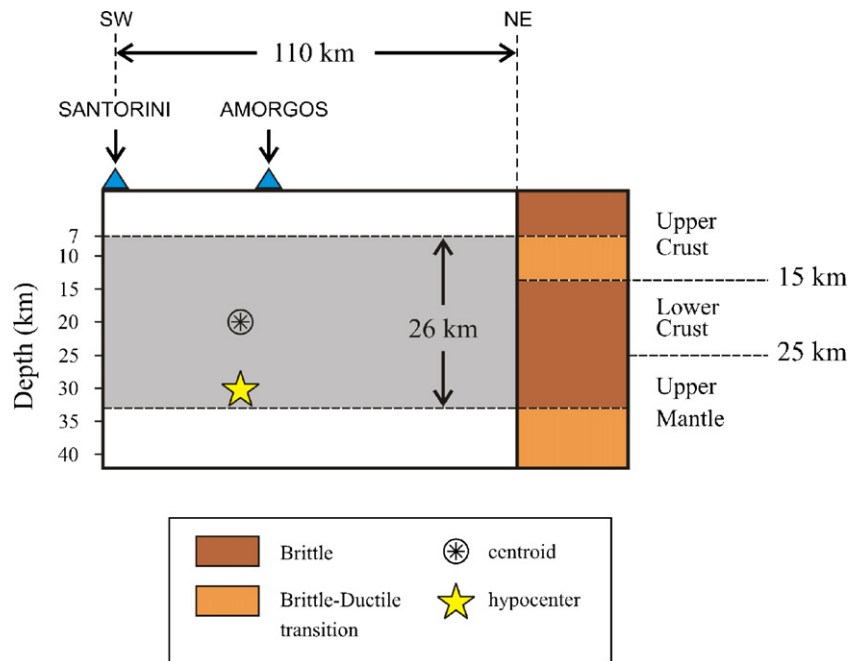


**Fig. 8.** Rupture scenario of the 1956 Amorgos earthquake based on all the available observations and rheological modelling presented in this study. Grey shaded area indicates the possible extent of the rupture zone. The column at the right hand side of the plot shows the rheological stratification of the area.

peratures of  $900^{\circ}\text{C}$  for the Cretan Sea and about  $1000^{\circ}\text{C}$  for the Cyclades islands. These temperatures are again in agreement with a surface heat flow of  $62\text{ mW m}^{-2}$  whose geotherm predicts  $984^{\circ}\text{C}$  at 60 km depth, while higher surface heat flow would result in a temperature of  $1176^{\circ}\text{C}$  or higher. These results imply that surface heat flow is lower than expected near the area of the Amorgos rupture zone, but probably increases locally around centers of active volcanism such as Santorini.

### 5.3. Effective viscosity of the lower crust

The relatively flat Moho detected beneath the southern Aegean has been explained by many authors as the result of lower crustal flow that allowed the Moho to remain flat during continuing extension (e.g., Tirel et al., 2004). This requires that the viscosity of the lower crust is low enough ( $< 10^{21}\text{ Pa s}$ ) so that such a flow can occur (Al-Zoubi and ten Brink, 2002). It is an open question posed by many authors whether the lower crust can still flow or not. The results of this study can be used to clarify this point further by utilizing the preferred rheological profile that consisted of a dry lower crust and a wet upper mantle. The effective viscosity is defined as  $n = \Delta\sigma/\dot{\epsilon}$  where  $\Delta\sigma$  is differential stress,  $\dot{\epsilon}$  is the strain rate and can be easily calculated as a function of depth (Fig. 9).

It can be seen that for the area around Amorgos the lower crust attains viscosity values of the order  $10^{23}\text{ Pa s}$  which is much higher than the critical value that would allow it to flow. Strain rates smaller than the ones found near Amorgos ( $< 10^{-17}\text{ s}^{-1}$ ) that are more appropriate for the western Cyclades, would have the effect of further increasing the effective viscosity of the lower crust. These results are in agreement with two other studies: (a) Zhu et al. (2006) estimated the viscosity of the lower crust in the southern Aegean using a simple model of a fluid layer over a fluid half space; the authors found values higher than  $10^{21}\text{ Pa s}$  concluding that the lower crust should be strong and therefore cannot flow, and (b) Fischer (2006) used a finite element rheological model of the Aegean–Anatolian region in order to show that the lower crustal viscosity for the southern Aegean is between  $10^{21}$  and  $10^{23}\text{ Pa s}$ .

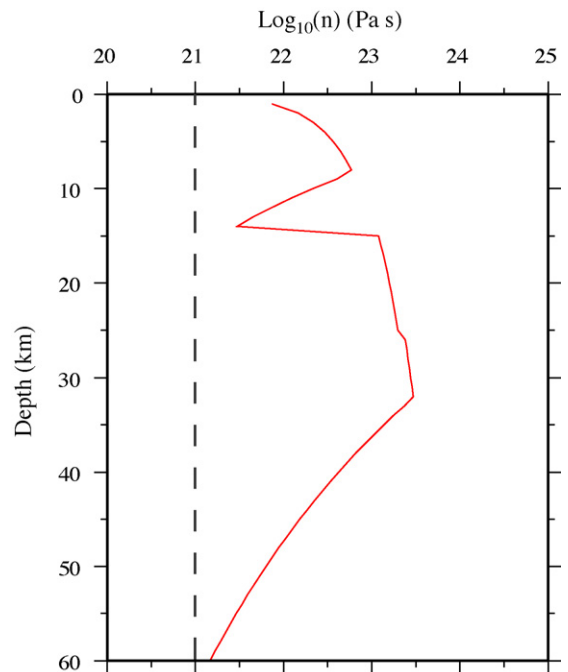


**Fig. 9.** Diagram showing the distribution of effective viscosity  $n$ , defined in the text, as a function of depth for the Amorgos–Santorini area. Viscosity values lower than the value highlighted by the vertical dashed line would allow the lower crust to flow over geological timescales.

Therefore, it seems that although the lower crust in the south Aegean could probably flow when the crust was thick and hot, it became progressively dry and lost this ability. This finding confirms the suggestion of McKenzie and Jackson (2002) that flow initiates when water-rich fluids drop the viscosity of the lower crust, but this effect is reversed once these fluids are removed from the rock matrix.

## 6. Conclusions

The main conclusions of this study can be summarized as follows:

- The lithosphere in the southern Aegean can be approximated by three layers representing the upper/lower crust and the upper mantle consisting of quartzite, diabase and peridotite respectively. This is based on seismic velocity models available for this area and is also consistent with densities inferred from gravity modelling.
- Surface heat flow in the area of the 1956 Amorgos earthquake of the order of  $62 \text{ mW m}^{-2}$  seems to be consistent with the Moho temperature derived from  $P_n$  seismic velocity and also with an independent study of thermal conditions in the European continent (Tesauro et al., 2009). This value may however, increase near areas of active volcanism such as Santorini island.
- A lithospheric rheology of wet quartzite/peridotite and dry diabase is favoured by the frequency–depth distribution of earthquakes and other geological observations. Such a stratification exhibits a strong upper mantle down to a depth of 33 km and a relatively weaker lower crust that is consistent with the well-known ‘jelly sandwich’ model. However, the effective viscosity of the lower crust is high enough ( $> 10^{21}$ ) to inhibit any kind of flow.
- A rupture scenario that emerges after considering the rheological conditions at Amorgos is that the 1956 event nucleated in the upper mantle, near the depth of peak strength. If the downdip width of the fault was about 26 km as calculated from empirical relationships, this means that the rupture would propagate only up to 7 km depth without reaching the seafloor. This agrees with recent modelling results of the 1956 tsunami which followed the earthquake and show that it was probably caused by secondary phenomena after the earthquake. A nucleation depth inside the upper mantle has also important implications for seismic hazard estimations since such earthquakes have longer recurrence periods than crustal events.

## Acknowledgements

I would like to thank the National Science Council of Taiwan for the financial support of this research. Constructive comments by two anonymous reviewers and the Editor-in-Chief Randall Stephenson helped to improve the original manuscript. Thanks are also due to Lupei Zhu, Wen-Tzong Liang and Sofia Rontogianni for useful discussions.

## References

Afonso, J.C., Ranalli, G., 2004. Crustal and mantle strengths in continental lithosphere: is the jelly sandwich model obsolete? *Tectonophysics* 394, 221–232, doi:10.1016/j.tecto.2004.08.006.

Albaric, J., Déverchère, J., Petit, C., Perrot, J., Le Gall, B., 2009. Crustal rheology and depth distribution of earthquakes: insights from the central and south East African System. *Tectonophysics* 468, 28–41, doi:10.1016/j.tecto.2008.05.021.

Aldersons, F., Ben-Avraham, Z., Hofstetter, A., Kissling, E., Al-Yazjeen, T., 2003. Lower-crustal strength under the Dead Sea basin from local earthquake data and rheological modeling. *Earth Planet. Sci. Lett.* 214, 129–142.

Al-Lazki, A.I., Sandvol, E., Seber, D., Barazangi, M., Turkelli, N., Mohamad, R., 2004.  $P_n$  tomographic imaging of mantle lid velocity and anisotropy at the junction of the Arabian, Eurasian and African plates. *Geophys. J. Int.* 158, 1024–1040, doi:10.1111/j.1365-246X.2004.02355.x.

Al-Zoubi, A., ten Brink, U., 2002. Lower crustal flow and the role of shear in basin subsidence: an example from the Dead Sea basin. *Earth Planet. Sci. Lett.* 199, 67–79.

Annen, C., Sparks, R.S.J., 2002. Effects of repetitive emplacement of basaltic intrusions on thermal evolution and melt generation in the crust. *Earth Planet. Sci. Lett.* 203, 937–955.

Black, P.R., Braille, L.W., 1982.  $P_n$  velocity and cooling of the continental lithosphere. *J. Geophys. Res.* 87, 10557–10568.

Bohnhoff, M., Rische, M., Meier, T., Becker, D., Stavrakakis, G., Harjes, H.-P., 2006. Microseismic activity in the Hellenic Volcanic Arc, Greece, with emphasis on the seismotectonic setting of the Santorini–Amorgos zone. *Tectonophysics* 423, 17–33, doi:10.1016/j.tecto.2006.03.024.

Brun, J.-P., Faccenna, C., 2008. Exhumation of high-pressure rocks driven by slab rollback. *Earth Planet. Sci. Lett.* 272, 1–7, doi:10.1016/j.epsl.2008.02.038.

Burov, E.B., Watts, A.B., 2006. The long-term strength of continental lithosphere: ‘jelly sandwich’ or ‘crème brûlée’? *GSA Today* 16, doi:10.1130/1052-5173(2006)016.

Casten, U., Snopek, K., 2006. Gravity modelling of the Hellenic subduction zone—a regional study. *Tectonophysics* 417, 183–200, doi:10.1016/j.tecto.2005.11.002.

Chen, W.-P., Molnar, P., 1983. Focal depths of intracontinental and intraplate earthquakes and their implications for the thermal and mechanical properties of the lithosphere. *J. Geophys. Res.* 88, 4183–4214.

Christensen, N.I., 1966. Elasticity of ultramafic rocks. *J. Geophys. Res.* 71, 5921–5931.

Christensen, N.I., Mooney, W.D., 1995. Seismic velocity structure and composition of the continental crust: a global view. *J. Geophys. Res.* 100, 9761–9788.

Déverchère, J., Petit, C., Gileva, N., Radziminovitch, N., Melnikova, V., San'kov, V., 2001. Depth distribution of earthquakes in the Baikal rift system and its implications for the rheology of the lithosphere. *Geophys. J. Int.* 146, 714–730.

Di Luccio, F., Pasyanos, M.E., 2007. Crustal and upper-mantle structure in the Eastern Mediterranean from the analysis of surface wave dispersion curves. *Geophys. J. Int.* 169, 1139–1152, doi:10.1111/j.1365-246X.2007.03332.x.

Endrun, B., Meier, T., Bischoff, M., Harjes, H.-P., 2004. Lithospheric structure in the area of Crete constrained by receiver functions and dispersion analysis of Rayleigh phase velocities. *Geophys. J. Int.* 158, doi:10.1111/j.1365-246X.2004.02332.x.

Endrun, B., Meier, T., Lebedev, S., Bohnhoff, M., Stavrakakis, G., Harjes, H.-P., 2008. S velocity structure and radial anisotropy in the Aegean region from surface wave dispersion. *Geophys. J. Int.* 174, 593–616, doi:10.1111/j.1365-246X.2008.03802.x.

Engdahl, E.R., van der Hilst, R.D., Buland, R.P., 1998. Global teleseismic earthquake relocation with improved travel time and procedures for depth determination. *Bull. Seism. Soc. Am.* 88, 722–743.

Fernández-Ibañez, F., Soto, J.I., 2008. Crustal rheology and seismicity in the Gibraltar Arc (western Mediterranean). *Tectonics* 27, TC2007, doi:10.1029/2007TC002192.

Fischer, K.D., 2006. The influence of different rheological parameters on the surface deformation and stress field of the Aegean–Anatolian region. *Int. J. Earth Sci.* 95, 239–249, doi:10.1007/s00531-005-0031-0.

Gomberg, J.S., Shedlock, K.M., Roecker, S.W., 1990. The effect of S-wave arrival times on the accuracy of hypocentre estimation. *Bull. Seism. Soc. Am.* 80, 1605–1628.

Handy, M.R., Brun, J.-P., 2004. Seismicity, structure and strength of the continental lithosphere. *Earth Planet. Sci. Lett.* 223, 427–441, doi:10.1016/j.epsl.2004.04.021.

Hollenstein, C., Müller, M.D., Geiger, A., Kahle, H.-G., 2008. Crustal motion and deformation in Greece from a decade of GPS measurements, 1993–2003. *Tectonophysics* 449, 17–40, doi:10.1016/j.tecto.2007.12.006.

Jackson, J., 2002. Strength of the continental lithosphere: time to abandon the jelly sandwich? *GSA Today* 12, 4–10, doi:10.1130/1052-5173(2002)012.

Jolivet, L., Faccenna, C., Piromallo, C., 2009. From mantle to crust: stretching the Mediterranean. *Earth Planet. Sci. Lett.* 285, 198–209, doi:10.1016/j.epsl.2009.06.017.

Jongsma, D., 1974. Heat flow in the Aegean. *J. R. Astr. Soc.* 37, 337–346.

Karagianni, E.E., Papazachos, C.B., Panagiotopoulos, D.G., Suhaldoc, P., Vuan, A., Panza, G.F., 2005. Shear velocity structure in the Aegean area obtained by inversion of Rayleigh waves. *Geophys. J. Int.* 160, 127–143, doi:10.1111/j.1365-246X.2005.02354.x.

Knapmeyer, M., Harjes, H.-P., 2000. Imaging crustal discontinuities and the down-going slab beneath western Crete. *Geophys. J. Int.* 143, 1–21.

Kreemer, C., Chamot-Rooke, N., 2004. Contemporary kinematics of the southern Aegean and the Mediterranean ridge. *Geophys. J. Int.* 157, 1377–1392, doi:10.1111/j.1365-246X.2004.02270.x.

Lamontagne, M., Ranalli, G., 1996. Thermal and rheological constraints on the earthquake depth distribution in the Charlevoix, Canada, intraplate seismic zone. *Tectonophysics* 257, 55–69.

Lee, W.H.K., Lahr, J.C., 1975. HYP071 (revised): a computer program for determining hypocenter, magnitude and first motion pattern of local earthquakes. *US Geol. Survey Open File Rep.*

Le Pichon, X., Angelier, J., 1979. The Hellenic arc and trench system: a key to the neotectonic evolution of the eastern Mediterranean area. *Tectonophysics* 60, 1–42.

Le Pichon, X., Chamot-Rooke, N., Lallemand, S., Noomen, R., Veis, G., 1995. Geodetic determination of the kinematics of central Greece with respect to Europe: implications for eastern Mediterranean tectonics. *J. Geophys. Res.* 100, 12675–12690.

Li, X., Bock, G., Vafidis, A., Kind, R., Harjes, H.-P., Hanka, W., Wylegalla, K., van der Meijde, M., Yuan, X., 2003. Receiver function study of the Hellenic subduction zone: imaging crustal thickness variations and the oceanic Moho of the descending African lithosphere. *Geophys. J. Int.* 155, 733–748.

Ma, K.F., Song, T.-R., 2004. Thermo-mechanical structure beneath the young orogenic belt of Taiwan. *Tectonophysics* 388, 21–31, doi:10.1016/j.tecto.2004.07.003.

Maggi, A., Jackson, J.A., MacKenzie, D., Priestley, K., 2000a. Earthquake focal depths, effective elastic thickness and the strength of the continental lithosphere. *Geology* 28, 495–498.

Maggi, A., Jackson, J.A., Priestley, K., Baker, C., 2000b. A re-assessment of focal depth distributions in southern Iran, the Tien-Shan and northern India: do earthquakes really occur in the continental mantle? *Geophys. J. Int.* 143, 629–661.

- Makris, J., 1978. The crust and upper mantle of the Aegean region from deep seismic soundings. *Tectonophysics* 46, 269–284.
- Makris, J., Stobbe, C., 1984. Physical properties and state of the crust and upper mantle of the eastern Mediterranean Sea deduced from geophysical data. *Mar. Geol.* 55, 347–363.
- McKenzie, D., Jackson, J., 2002. Conditions for flow in the continental crust. *Tectonics* 21, 1055, doi:10.1029/2002TC001394.
- McClusky, et al., 2000. Global positioning system constraints on plate kinematic and dynamics in the Eastern Mediterranean and Caucasus. *J. Geophys. Res.* 105, 5695–5719.
- Melis, N.S., Konstantinou, K.I., 2006. Real-time seismic monitoring in the Greek region: an example from the 17 October 2005 East Aegean Sea earthquake sequence. *Seism. Res. Lett.* 77, 364–370.
- Okal, E.A., Synolakis, C.E., Uslu, B., Kalligeris, N., Voukouvalas, E., 2009. The 1956 earthquake and tsunami in Amorgos, Greece. *Geophys. J. Int.* 178, 1533–1554, doi:10.1111/j.1365-246X.2009.04237.x.
- Papazachos, B.C., Koutitas, C., Hatzidimitriou, P.M., Karakostas, B.G., Papaioannou, C.A., 1985. Source and short-distance propagation of the July 9, 1956 southern Aegean tsunami. *Mar. Geol.* 65, 343–353.
- Papazachos, B.C., Papazachou, K., 1997. *The Earthquakes of Greece*, Ziti editions, Thessaloniki.
- Papazachos, B.C., Karakostas, V.G., Papazachos, C.B., Scordilis, E.M., 2000. The geometry of the Wadati-Benioff zone and lithospheric kinematics in the Hellenic arc. *Tectonophysics* 319, 275–300.
- Papazachos, C., Nolet, G., 1997. P and S velocity structure of the Hellenic area obtained by robust nonlinear inversion of travel times. *J. Geophys. Res.* 102, 8349–8367.
- Priestley, K., Jackson, J., McKenzie, D., 2008. Lithospheric structure and deep earthquakes beneath India, the Himalaya and southern Tibet. *Geophys. J. Int.* 172, 345–362, doi:10.1111/j.1365-246X.2007.03636.x.
- Ranalli, G., Murphy, D.C., 1987. Rheological stratification of the lithosphere. *Tectonophysics* 132, 281–295.
- Ranalli, G., 1995. *Rheology of the Earth*. Chapman & Hall, London.
- Sachpazi, M., Hirn, A., Narsessian, A., Avedik, F., McBride, J., Loucoyannakis, M., Nicolich, R., 1997. A first coincident normal-incidence and wide-angle approach to studying the extending Aegean crust. *Tectonophysics* 270, 301–312.
- Schenkova, Z., Kalogeras, I., Schenk, V., Pichl, R., Kourouzidis, M., Stavrakakis, G., 2005. *Atlas of Isoseismal Maps of Selected Greek Earthquakes (1956–2003)*. Evonymos Ecological Library, Athens.
- Sibson, R.H., 1984. Roughness at the base of the seismogenic zone: contributing factors. *J. Geophys. Res.* 89, 5791–5799.
- Sodoudi, F., Kind, R., Hatzfeld, D., Priestley, K., Hanka, W., Wylegalla, K., Stavrakakis, G., Vafidis, A., Harjes, H.-P., Bohnhoff, M., 2006. Lithospheric structure of the Aegean obtained from P and S receiver functions. *J. Geophys. Res.* 111, B12307, doi:10.1029/2005JB003932.
- Solaro, G., Tizzani, P., Milano, G., Pauselli, C., 2007. Rheological behaviour of the crust in the southern Apennine (Italy): results from a thermal and seismological study. *Terra Nova* 19, 353–359, doi:10.1111/j.1365-3121.2007.00759.x.
- Tesauro, M., Kaban, M.K., Cloetingh, S.A.P.L., 2009. A new thermal and rheological model of the European lithosphere. *Tectonophysics* 476, 478–495, doi:10.1016/j.tecto.2009.07.022.
- Tirel, C., Gueydan, F., Tiberi, C., Brun, J.-P., 2004. Aegean crustal thickness inferred from gravity inversion: geodynamical implications. *Earth Planet. Sci. Lett.* 228, 267–280, doi:10.1016/j.epsl.2004.10.023.
- Tsokas, G.N., Hansen, R.O., 1997. Study of the crustal thickness and the subducting lithosphere in Greece from gravity data. *J. Geophys. Res.* 102, 20585–20597.
- Wells, D.L., Coppersmith, K.J., 1994. New empirical relationships among magnitude, rupture length, rupture width, rupture area, surface displacement. *Bull. Seism. Soc. Am.* 84, 974–1002.
- Zellmer, G., Turner, S., Hawkesworth, C., 2000. Timescales of destructive plate margin magmatism: new insights from Santorini, Aegean volcanic arc. *Earth Planet. Sci. Lett.* 174, 265–281.
- Zhu, L., Mitchell, B.J., Akyol, N., Cemen, I., Kekovali, K., 2006. Crustal thickness variations in the Aegean region and implications for the extension of continental crust. *J. Geophys. Res.* 111, B01301, doi:10.1029/2005JB003770.